Analyst

Two-dimensional Identification and Localization of Isomers in Crystallin Peptides Using TWIM-MS

Journal:	*Analyst*
Manuscript ID	AN-ART-05-2020-001036.R1
Article Type:	Paper
Date Submitted by the Author:	22-Jun-2020
Complete List of Authors:	Wu, Hoi-Ting; University of California Riverside Julian, Ryan; University of California Riverside

SCHOLARONE™
Manuscripts

1
2
3
4
5
6
7
8
9
10
11
12
13
14
15
16
17
18
19
20
21
22
23
24
25
26
27
28
29
30
31
32
33
34
35
36
37
38
39
40
41
42
43
44
45
46
47
48
49
50
51
52
53
54
55
56
57
58
59
60

Two-dimensional Identification and Localization of Isomers in Crystallin Peptides Using TWIM-MS

Hoi-Ting Wu, Ryan R. Julian *

Department of Chemistry, University of California, Riverside, California 92521, United States

Corresponding Author

* Correspondence should be sent to: ryan.julian@ucr.edu

Department of Chemistry, University of California, Riverside, 501 Big Spring Road, Riverside, California 92521, United States, (951)827-3959

1
2
3
4
5
6
7
8
9
10
11
12
13
14
15
16
17
18
19
20
21
22
23
24
25
26
27
28
29
30
31
32
33
34
35
36
37
38
39
40
41
42
43
44
45
46
47
48
49
50
51
52
53
54
55
56
57
58
59
60

Abstract

Recent studies have illuminated connections between spontaneous chemical reactions that cause isomerization at specific protein residues and various age-related diseases including cataracts and Alzheimer's. These discoveries provide impetus for better analytical methods to detect and characterize isomerization in proteins, which will enable a more complete understanding of the underlying relationship between these modifications and biology. Herein we employ a two-dimensional approach for identification of peptides isomers that also includes pinpointing of the modified residue. Collision-induced dissociation is used to fragment ions in the first dimension, followed by separation of the fragments with travelling-wave ion mobility. By comparing data obtained from both isomers, differences in either fragment-ion intensities or arrival-time distributions can be used to identify isomeric forms and the specific site of modification within the peptides. Synthetic peptide standards with sequences derived from long-lived proteins in the eye lens and isomerization at serine, aspartic acid, and glutamic acid were examined. Although both dimensions are capable of isomer identification, ion mobility is much better at determining the site of modification. In general, separation of isomeric forms by ion mobility is possible but does not follow predictable trends dictated by sequence or fragment-ion length. In most cases, however, the site of isomerization can be precisely determined.

1
2
3
4
5
6
7
8
9
10
11
12
13
14
15
16
17
18
19
20
21
22
23
24
25
26
27
28
29
30
31
32
33
34
35
36
37
38
39
40
41
42
43
44
45
46
47
48
49
50
51
52
53
54
55
56
57
58
59
60

Introduction

Recent reports including studies on aging and neurochemistry have highlighted the biological importance of isomerized residues in proteins and peptides.[1-4] While most proteins are recycled quickly in cells, long-lived proteins (LLPs) can persist for months or years.[5] Over this time, LLPs are subject to traditional post-translational modifications (PTMs), including phosphorylation, oxidation, and glycosylation.[6,7,8] In addition, LLPs are much more prone to spontaneous chemical modifications (SCMs) than proteins that turnover quickly. Among the most common SCMs are isomerization and epimerization of individual residues, which are particularly difficult to characterize because they do not shift mass or any other easily identifiable metric. Epimerization occurs when one amino acid converts from the L to D configuration. Isomerization is primarily applicable to aspartic acids (Asp) residues via the well-known pathway outlined in Scheme 1.[9,10] Although these modifications are subtle in some ways, they can have dramatic consequences, such altering the behavior of crystallin proteins in the eye lens, triggering receptors in the brain, or interfering with digestion in the lysosome. [2,11,12,13,14]

Aspartic acid (Asp) and Serine (Ser) are most susceptible to isomerization in human LLPs.[15] Asp isomerization yields four end products as shown in Scheme 1. Glutamic acid (Glu) can also produce four isomers in a similar fashion, though at a much slower pace.[16] Modification of Ser occurs through epimerization of the side chain from the L- to D-chirality. The mechanism has not been experimentally confirmed, though proposals have been made.[17] Numerous experiments on the eye lens have demonstrated that modifications of Asp and Ser are abundant over timespans of years.[12,15,18] Additional in vitro experiments have demonstrated that shorter timescales (weeks to months) can accommodate accumulation of Asp isomerization in disordered molecules.[1] Unfortunately, traditional proteomics approaches are essentially blind to isomerization and epimerization, which has spawned the development of more targeted approaches for their characterization.
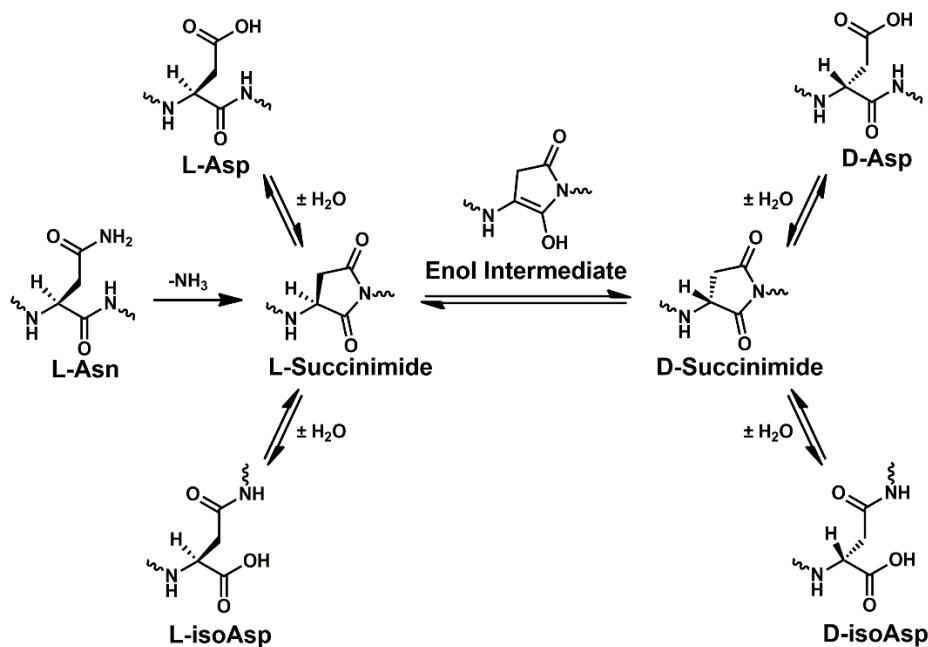
Scheme 1 Isomerization of Asp and deamidation of Asn can produce four Asp isomers through a succinimide intermediate.

Isomerization and epimerization do not change mass, but they can be detected by fragmentation in MS/MS experiments. Differences in fragmentation patterns have been observed for collision-induced dissociation (CID), electron-captured dissociation (ECD),[19,20] and radical-directed dissociation (RDD).[21-22] Although comparing fragmentation patterns is a straightforward method to identify isomers, it is not without limitations. First, the success of the analysis depends on the structural sensitivity of the fragmentation method. CID is the most commonly available but yields the poorest results. RDD is the most structurally sensitive but requires photodissociation, which is not widely available. In addition, the isomers must be analyzed separately, meaning that examination of a biological sample is typically preceded by separation with liquid chromatography. Incomplete separation can complicate identification, particularly for methods with poor structural sensitivity.[23] However, the biggest drawback is that fragmentation does not typically reveal the location of the modification. This problem can be

solved by comparing dissociation with a synthetic standard, but for complex peptides with multiple isomerization sites, this can necessitate synthesis of dozens of peptides.

Recently, ion mobility spectrometry coupled with mass spectrometry (IMS-MS) has become a popular option for analysis of peptides. IMS separates ions based on their collision-cross sections which are a function of their mobility in a buffer gas (H_2, He, or N_2).[24] IMS can differentiate peptide epimers[25,26] and D/L-Asp and isoAsp isomers in Aβ.[27,28] However, examination of intact peptides only confirms the presence of isomeric forms, synthetic peptides are still necessary to locate the isomerized residue. To overcome these limitations, Li and coworkers separated CID fragment ions with IMS and used shifts in arrival time to locate epimerized residues.[29] In their experiments, all fragment ions containing epimerized residues experienced shifts in arrival time relative to canonical fragments. The ability to localize modification site is a significant breakthrough, but these experiments focused on neuropeptides that are isomerized at a uniform position. Isomerized residues occurring in LLPs can be found anywhere in the peptide sequence and can adopt more than two forms.

Herein, we seek to identify and localize isomerized residues, such as Ser, Asp, and Glu, at different locations in the crystallin peptides using the shifts in the mobility of fragment ions produced by CID. In addition, we explore whether changes in CID fragment intensity can be used to locate isomerized sites, providing a second dimension for examination.

Experimental Section

Materials. Organic solvents and reagents were purchased from Fisher Scientific and Sigma-Aldrich (St. Louis, MO) and used without further purification. FMOC-protected amino acids and Wang resin were purchased from Anaspec, Inc. (Fremont,CA) or Chem-Impex International. Glu isomers were purchased from CarboSynth.

Peptide Synthesis. Peptides were synthesized manually following an accelerated FMOC-protected solid-phase peptide synthesis protocol.[30] Peptides were stored frozen in 50/50 acetonitrile/water(v/v).

Analysis. 10µM of the peptide standard was prepared in 49.5/49.5/1.0 acetonitrile/water/formic acid (v/v/v). Experiments were performed on a Waters Synapt G2-Si mass spectrometer. The peptide sample was directly injected using a standard electrospray source. Peptides were fragmented in the pre-mobility trap by adding a bias of 80-110V. Other instrument acquisition parameters were as follows: inlet capillary voltage of 1.5 kV, sampling cone setting of 40V, and source temperature of 150ºC. The argon gas pressures in the traveling wave ion guide trap and the traveling wave ion guide transfer cell were 2.48E-2 and 2.57E-2 mbar. The wave height, the wave velocity, and the nitrogen pressure in the traveling wave guide were 40V, 1000m/s, and 2.85mbar. Three replicates were collected for each peptide isomer. Data processing was conducted using Waters MassLynx 4.1 to extract the CID intensity and ATDs for each set of fragment ions. The ATDs were smoothed using Savitzky Golay with a window size of 1 scan and 1 smooth in MassLynx before data extraction.

Results & Discussion

Strategy for identification and localization of isomerized residues in peptides. Our workflow and data analysis to identify and locate isomerized residues in peptides is summarized in Figure 1. First, peptides are isolated and fragmented prior to separation by ion mobility. The resulting spectrum contains arrival-time distributions (ATDs) for all fragment ions as shown in Figure 1a. The mass of each fragment can be used to extract out the ATD for each ion, as shown in Figure 1b. To compare ATDs for the same fragment ions derived from different isomers of the same peptide sequence, the area overlap between the respective ATDs is calculated as shown in Figure 1c. We also explored comparing ATDs by peak maxima or weighted averages but found those methods were more prone to error. ATDs with flattened tops can yield differing maxima

that are not statistically significant (Figure S1). Weighted averages may solve this issue, but can also overlook the presence of alternate conformations that could potentially vary between isomers. Smaller area overlap indicates that ions are less structurally similar, making them more likely to contain isomerized residues.
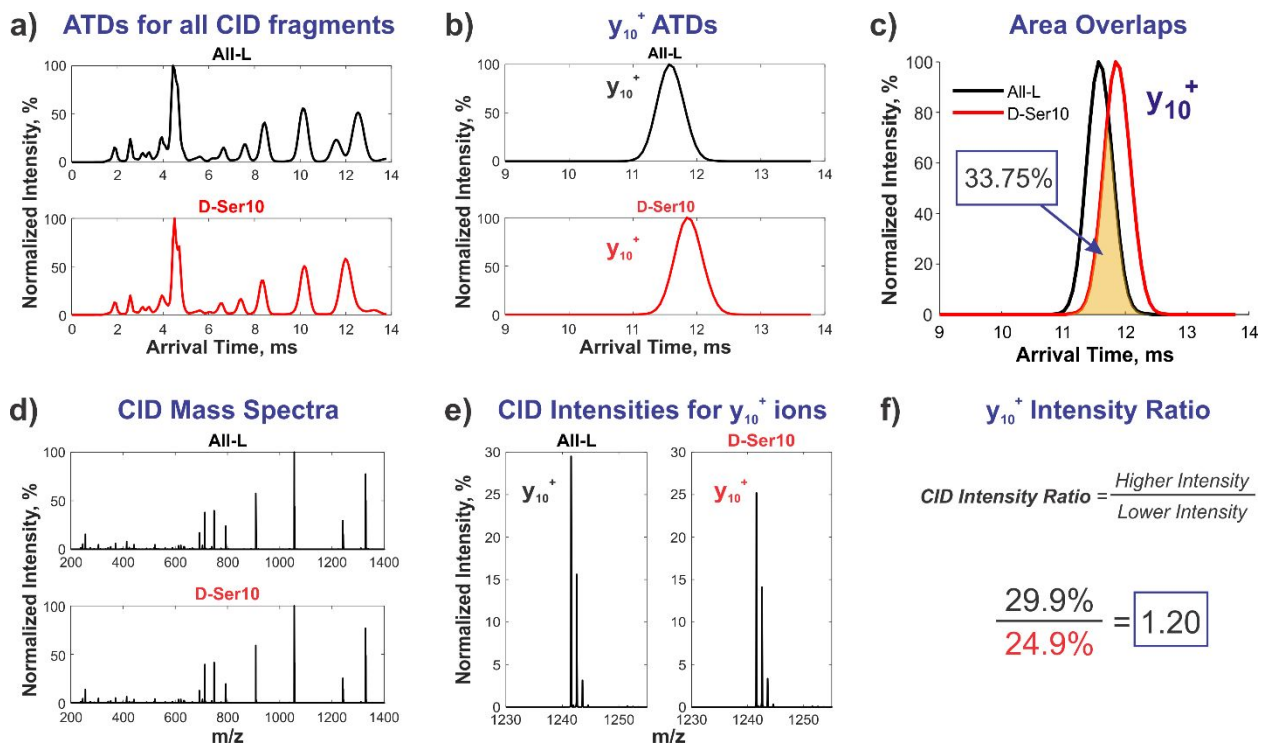

Figure 1 Summary of the workflow and data analysis for the two-dimensional identification and localization of the isomer in peptides. This data is derived from the APSWFDTGLSEMR peptides, the sidechain of Ser10 is epimerized in this example.

Because ions are fragmented during data acquisition, CID spectra (Figure 1d) are generated simultaneously with ATDs. Differences in fragment-ion intensities can also be used to identify isomers, as discussed above. Typically, R-values derived from the greatest differences in fragment intensities are employed for quantifying differences between isomers.[22,31-32] Our interest in this study is to evaluate whether differences in fragment intensity provide information about the site of modification. Therefore, for each fragment ion extracted (Figure 1e), the ratio of

the most abundant isotope from each isomer will be calculated according to Equation (1).

$$\text{CID Intensity Ratio} = \frac{\text{higher intensity}}{\text{lower intensity}} \qquad (1)$$

The numerator is set as the higher intensity fragment so that the ratio will always be greater

than or equal to 1. The CID intensity ratios are calculated for all fragment ion pairs where ATDs

are compared, providing a second dimension of data.

To establish statistically relevant thresholds for differentiating both ATD area-overlaps and

CID intensity ratios, thresholds were calculated at the 99% confidence interval based on

standard deviations of replicate data obtained from the same peptide (e.g. All-L vs. All-L for

each peptide listed in Table 1). For each individual data point obtained from one isomer, the

average value is reported with the standard deviation as error bars for both ATD area-overlaps

and CID intensity ratios. If the ATD area-overlap for an ion is below the threshold, it signifies

that the isomers produced fragments with differing structures. If the CID intensity ratio is above

the threshold, it signifies that the abundance of that fragment ion varied significantly between

isomers.

Table 1. Synthetic peptide isomers assessed in this study.

Peptide Sequence	Source Protein	Isomerized Residue
APSWFDTGLSEMR	Human αB-crystallin, 57-69	All-L
		D-Ser3
		D-Ser10
GYQYLLEPGDFR	Human βB1-crystallin, 202-213	L-Asp
		D-Asp
		D-isoAsp
		L-isoAsp
HFSPEDLTVK	Human αA-crystallin, 79-88	All-L
		D-Asp
		D-isoAsp
		L-isoAsp
		D-Glu
		D-isoGlu
		L-isoGlu

D/L-Ser Epimers. The list of peptides examined in this study is provided in Table 1. All sequences are derived from crystallin proteins that are LLPs in the eye lens. Epimerization of the Ser sidechain is one of the most abundant forms of isomerization in LLPs.[7] Furthermore, the sidechain of Ser is small, which should make differences in collision-cross section difficult to detect. The APSWFDTGLSEMR peptide, found in αB-crystallin 57-69, has two serine residues (Ser3 and Ser10) that epimerize. CID of the [M+2H]$^{2+}$ precursor ion produces mainly b- and y-ions, as expected (Figure S2). Data analysis as described above is shown for the Ser3 epimers in Figure 2. The ATD area-overlaps for the series of b-ions are shown in Figure 2a. Although epimerization is located at Ser3, structural differences in the b-ions are not observed until two residues later in the b_5 ion. Most of the remaining b-ions are below the threshold (red dotted line), indicating that structural differences can be detected. Collectively, the data in Figure 2a indicates the location of the isomer is within the first five residues of the peptide (^{1}APSWF^5). Figure 2b shows the area-overlaps of singly (blue) and doubly charged (orange) y-ions of the Ser3 epimers. The singly charged y-ions do not show any structural differences from y_2 to y_{10}, which is consistent with the fact that they do not contain the modified site, Ser3. However, the $y_{11}{}^+$ ion does contain the modified site, but both epimers have nearly identical ATDs. In contrast, the doubly charged y-ions follow an ideal pattern where all ions containing the modified sites have low ATDs overlap while all of the ions lacking Ser3 have similar ATDs overlap. Unfortunately, it is clear that fragments containing Ser3 may yield either identical or dissimilar ATD overlaps, meaning that *instances where overlap is high are not diagnostic*. Therefore, only fragments below the threshold can be used to identify the site of modification. Combining the results from all b- and y-ions confines the isomerized location to three residues (^{3}SWF^5).

The CID intensity ratios for the Ser3 epimers, AP\underline{S}WFDTGLSEMR, are shown in Figure 2c and 2d. All of the observed ratios are close to 1, indicating small differences between the CID spectra for the two epimers. Although some of the ratios are above the 99% threshold and

therefore statistically significant, it should be pointed out that these are highly averaged results

taken from direct infusion of purified samples. It is unlikely that these differences would be

observable in examination of actual biological samples. In any case, the observed dissimilarities

in fragmentation do not appear to point out the location of the modification.

Results for the Ser10 epimers of the same sequence, APSWFDTGL$\underline{S}$EMR, are shown in

Figure 3. For these peptides, idealized behavior is observed for the singly charged b-ions,

where no differences are observed for fragments missing Ser10 and all fragments containing

Ser10 are structurally distinct. These ions locate the epimerization site at or before Ser10 (i.e.

within ^{1}APSWFDTGLS^{10}). ATD overlaps for the singly and doubly charged y-ions are shown in

Figure 3b. Sequence coverage for the doubly charged ions is low and provides no additional

information not found in the singly charged ions. The y-ions reveal no structural differences

before y_4^+, isolating the modification site in the final four residues. Interestingly, the structural

differences are significant for most of the y-ions with the exception of the y_9 ion, which has a

much higher degree of overlap for both the singly and doubly charged ions. Combining both b-

and y-ions, the epimerization location is narrowed down to a single residue, Ser10. Again, the

CID intensity ratios for b- and y-ions are similar and do not appear to reveal any information

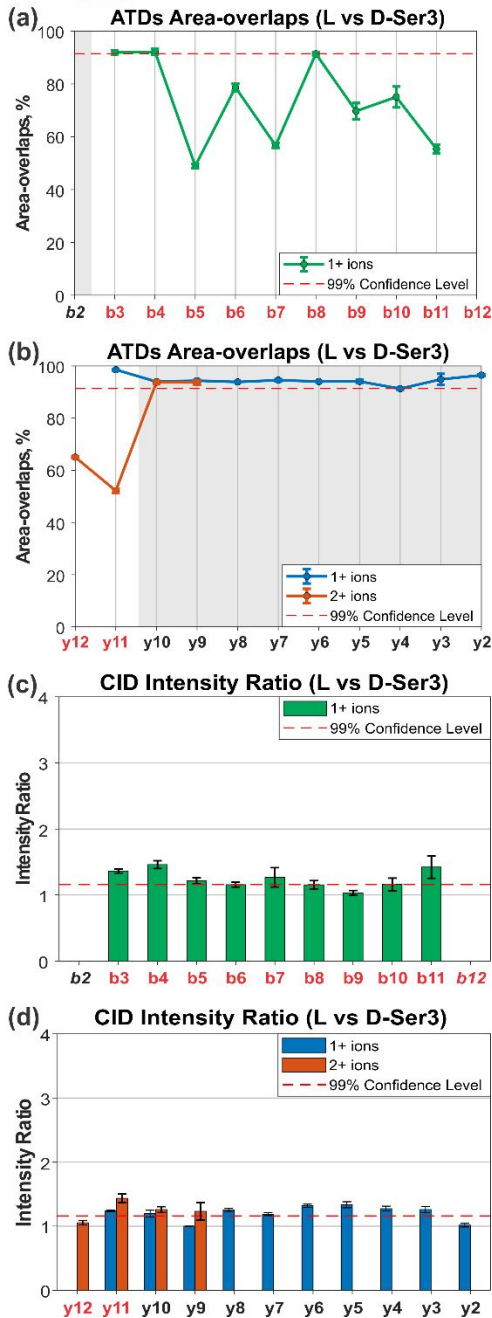about the location of the modified Ser.

Figure 2 ATD area-overlaps from the Ser3 epimers D/L-AP<u>S</u>WFDTGLSEMR. **(a)** b-ions and

(b) singly charged (blue) and doubly charged (orange) y-ions. Fragment ions labeled in Italic are

not observed in the data. CID intensity ratios of the isomeric **(c)** b-ions and **(d)** singly charged

(blue) and doubly charged (orange) y-ions. The error bars indicate the variations of the results in

three experimental replicates. The dashed red line indicates the 99% confidence level in both

area-overlaps in ATDs and CID intensity ratios.
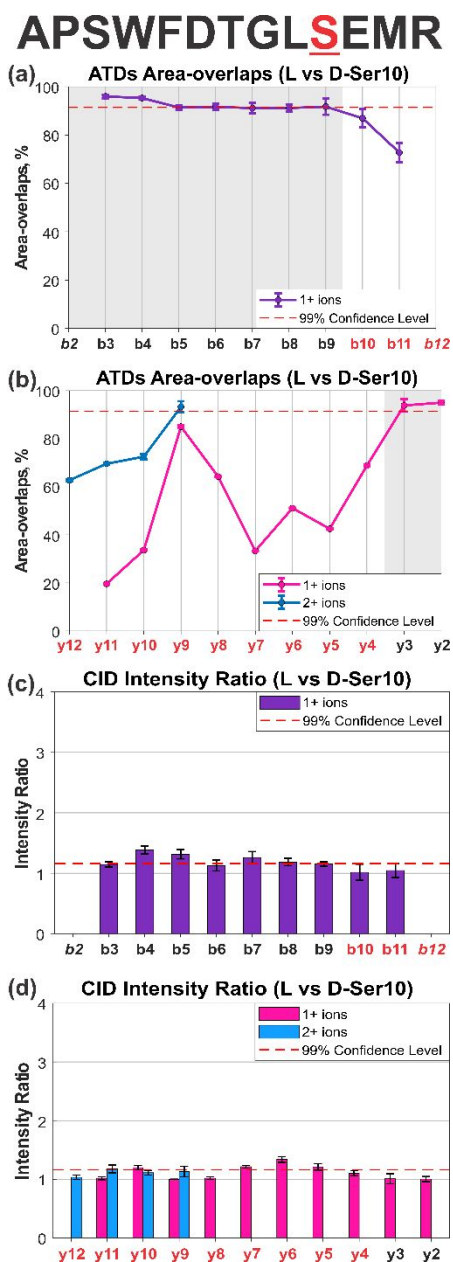
Figure 3 ATD area overlaps in the **(a)** b-ions and **(b)** singly charged (pink) and doubly

charged (blue) y-ions, CID intensity ratios of the isomeric **(c)** b-ions and **(d)** singly charged

(pink) and doubly charged (blue) y-ions from the Ser10 epimers of D/L-APSWFDTGLSEMR.

Aspartic Acid Isomers. As illustrated in Scheme 1, Asp populates four isomeric forms. The existence of four isomers complicates analysis because comparison between each form relative to every other form is necessary. This leads to a total of six comparison values for each fragment for a peptide with a single Asp, as illustrated by the results for GYQYLLEPGDFR (found in βB-crystallin 202-213) shown in Figure 4. Figure 4a shows the ATD area-overlaps for singly charged y-ions. Overlap relative to the L-Asp isomer diverges at y_3 with respect to all other isomers (see blue lines). The D-Asp isomer loses overlap relative to the iso-Asp forms at y_4 (orange lines). Finally, the overlap of D-isoAsp relative to L-isoAsp diverges at y_5 (green line). This data reveals the existence of four isomers within the C-terminal PGDFR part of the peptide, which would strongly suggest isomerization of Asp if the data had been collected from a biological source because the remaining residues are not prone to isomerize. The b-ions are all within the overlap threshold and reveal no structural differences (Figure S4a). Results for the doubly charged y-ions are shown in Figure 4b. Interestingly, all ions are overlapped for the y_4^{2+} ion, yet none are overlapped for the y_5^{2+} ion. The relative degree of overlap between isomers does not remain consistent among fragment ions (i.e. the lines in Figure 4a and 4b crisscross in a haphazard fashion), suggesting that a complex relationship exists between collision-cross section and isomeric form.

The CID intensity ratios relative to L-Asp are shown for the singly and doubly charged ions in Figure 4c and 4d, respectively. Interestingly, the abundance of the y_3^+ ion varies significantly between L/D-Asp and L/D-isoAsp. This suggests that the iso-configuration may influence fragmentation leading to y-ion formation, potentially providing information about the site of isomerization. Unfortunately, for the doubly charged ions y_3^{2+} is not observed, and no significant other differences are noted (see Figure 4d).
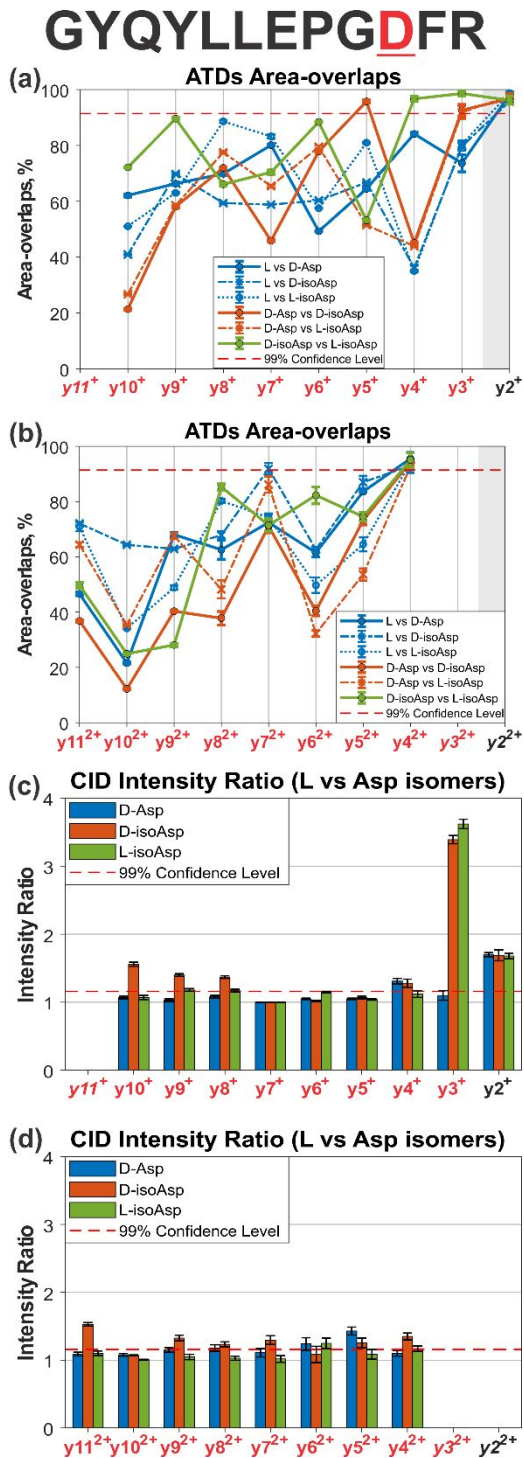
Figure 4 Results for Asp isomers of GYQYLLEPGD̲FR. ATD area-overlaps between L-Asp and D-Asp (blue), D-isoAsp (orange), or L-isoAsp (green) for (a) singly charged y-ions and (b) doubly charged y-ions. CID intensity ratios of the isomeric (c) singly charged y-ions and (d) doubly charged y-ions.

Results for HFSPE<u>D</u>LTVK (found in αA-crystallin 79-88) are shown in Figure 5. Figure 5a shows the ATD area-overlaps for the series of b-ions. Overlaps relative to most Asp isomers start to diverge at b_6, though the isomer pairs L-Asp/L-isoAsp and D-Asp/D-isoAsp are not differentiable. D-Asp relative to D-isoAsp no longer overlap at b_7 ion, but L-Asp cannot be separated from L-isoAsp for any of the b-ions. The results suggest that the isomerized site is within the N-terminal HFSPED part of the peptide. ATD area-overlaps for y-ions are shown in Figure 5b. All ions overlap for y_2 through y_4, as expected because these residues do not contain the isomerized site. All ion pairs diverge at y_5 with the exception of L-Asp versus D-isoAsp, which become differentiable at y_6. Area overlaps vary by ion but remain low until y_9, where all pairs exhibit greater overlap though some are still below threshold. Combined data from the b- and y-ions strongly indicate Asp as the site of isomerization.

The CID intensity ratios relative to L-Asp are shown for both b- and y-ions in Figure 5c and 5d. The CID intensity ratios for the b-ions are all close to 1, suggesting that structural differences among isomers do not significantly influence fragmentation for b-ions. However, the variations in CID intensity ratios for y-ions may allow for probing the isomerized site. Interestingly, greater variation is noted in the y-ions as shown in Figure 5d. Again, differences are noted between the canonical and iso-Asp forms for the y_6 through y_4 fragment ions. The greatest difference is observed for y_5, where cleavage occurs on the N-terminal side of the isomerized Asp residues. Intensities for L/D-Asp and L/D-isoAsp pairs contrast near the isomerized site. This observation further supports the idea that the iso-configuration may impact the formation of y-ions, possibly providing clues about the location of modifications in unknown systems.
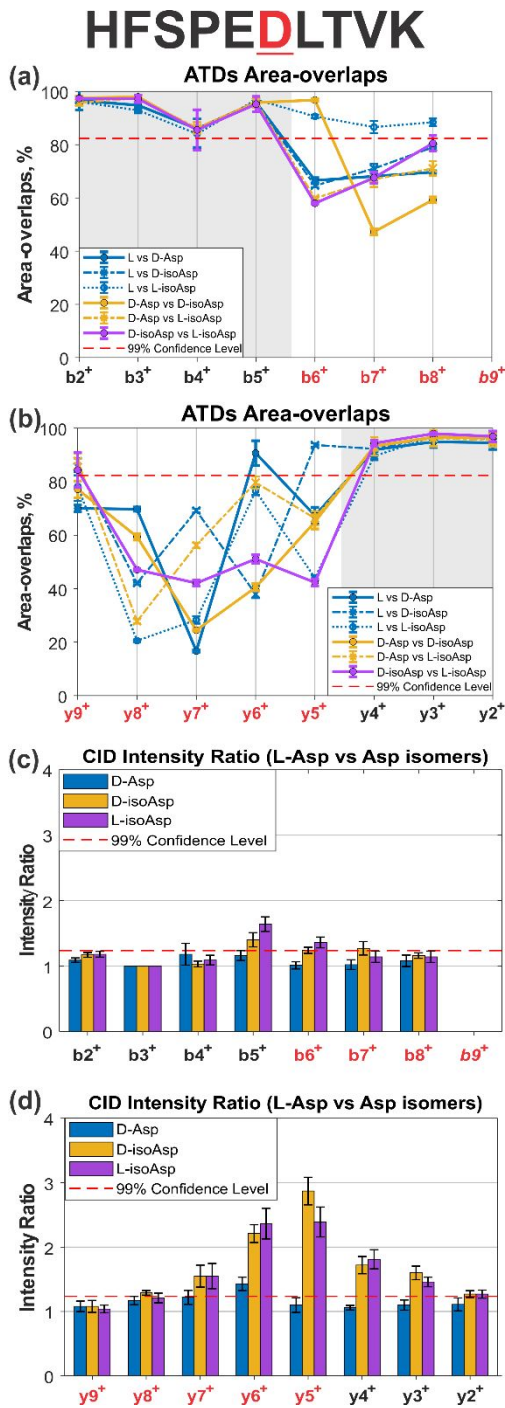
Figure 5 Result summary for Asp isomers of HFSPE<u>D</u>LTVK, L-Asp vs D-Asp (blue), D-isoAsp (yellow), or L-isoAsp (purple). ATD area overlaps in the isomeric (a) b-ions and (b) y-ions. CID intensity ratios of the isomeric (c) b-ions and (d) y-ions.

Glutamic Acid Peptide Isomers. Glutamic acid (Glu) also populates four isomeric forms through isomerization pathways analogous to those described for Asp.[16] Therefore, six comparisons for each fragment are also required for Glu isomers. Figure 6 illustrates results for HFSPEDLTVK, part of αA-crystallin 79-88.[13] ATD area-overlaps for singly charged b-ions are shown in Figure 6a. Area-overlaps relative to L-Glu and D-Glu separate at b_5 with respect to all other isomers, but the isoGlu isomers are not distinguishable until the b_6 ion. The data suggests the location of the isomerized residue is within the N-terminal HFSPE part of the peptide. Results for the singly charged y-ions are displayed in Figure 6b. Although some separation is noted at y_6, more noticeable differences are observed starting with y_7 for most isomers. The exception to this trend is noted for L-isoGlu relative to L-Glu, which are largely overlapped for most ions, with the least overlap observed in the final ion in the series, y_9. Additionally, b_4 does not contain the isomerized site yet D-Glu relative to D-isoGlu in Figure 6a lies just below the threshold. These results likely represent an example of the 1% error relative to the 99% threshold rather than bona fide structural differences.

The CID intensity ratios relative to L-Glu are shown for b- and y-ions in Figure 6c and 6d. Interestingly, the CID intensity ratios for all Glu isomers relative to L-Glu are significantly above the 99% threshold at the isomerized site for both b- and y-ions. Unlike Asp isomers, both D-Glu and the D/L-isoGlu CID intensities are distinct relative to L-Glu at the site of isomerization. These results suggest that both the iso-configuration and the side chain stereochemistry influence fragmentation for this peptide. Further experiments will be required to determine if this is a generally applicable phenomenon for Glu-isomers, or if the particular gas-phase structure for this sequence is responsible for the behavior.
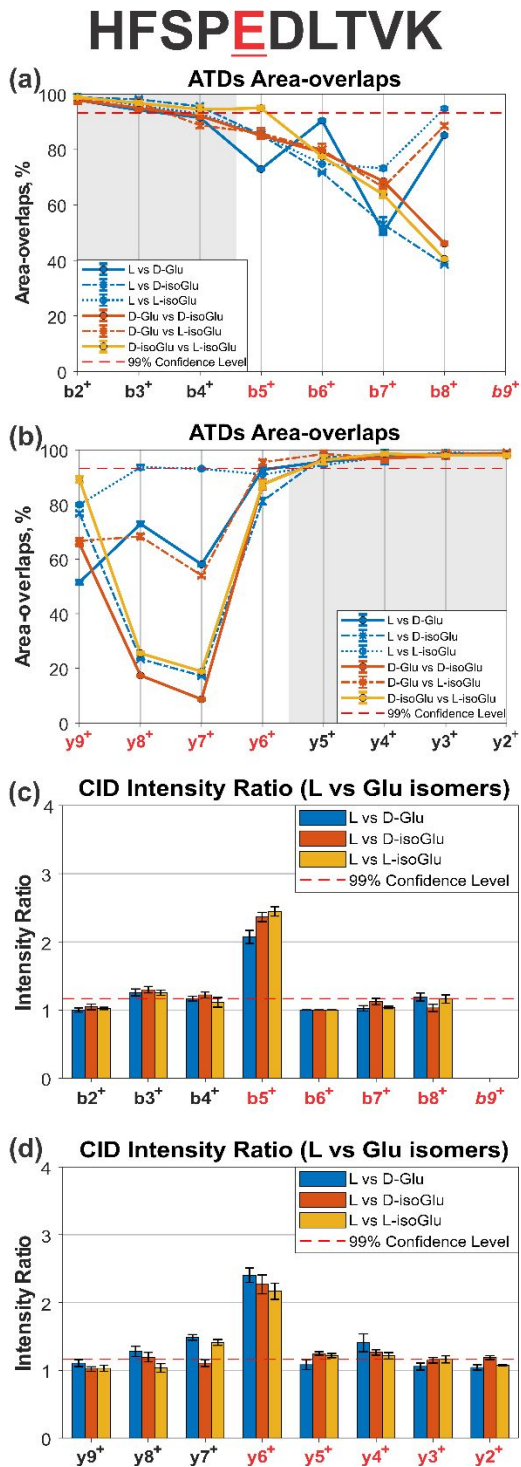
17

Figure 6 Result summary for Glu isomers HFSP<u>E</u>DLTVK, L-Glu vs D-Glu (blue), D-isoGlu (orange), or L-isoGlu (yellow). ATD area overlaps in the isomeric **(a)** b-ions and **(b)** y-ions. CID intensity ratios of the isomeric **(c)** b-ions and **(d)** y-ions.

Collective Analysis. Above we provide detailed results examining the separation and identification of challenging examples of peptide isomers, but further information can be derived from a more collective analysis. First, in terms of isomer identification, comparison of ATD overlap is highly successful. Identification requires only that one ATD overlap lie below the threshold, which was easily achieved in every case. Furthermore, it should be noted that the precursor ions did not resolve in every case and that better separation could always be observed in one or more of the fragment-ion channels. An example of this is shown for HFSP$\underline{E}$DLTVK in Figure 7a, where the y_7 ion ATDs are obviously more distinct than the precursor. The most likely explanation for this observation is that in a fragment ion, the isomerized residue accounts for a larger portion of the overall structure.

This concept is explored further in Figure 7b, which illustrates the statistical distributions of ATD area overlap as a function of fragment size. Although size may help fragment ions adopt distinct structures more often than larger precursor ions, there is clearly a limit to this effect. For example, in case of single amino acids, identical collision-cross sections will be obtained. In Figure 7b, it is clear that fragments containing only 3 residues are also too small to effectively separate. This suggests that 4 residues are required to accommodate intramolecular interactions that lead to differences in ATD. The range of ATD area overlaps is typically broad, with slightly favored sizes clustering every three residues at 4, 7, and 10 amino acids in length. This trend may be coincidental, or may imply that certain fragment lengths allow for additional intramolecular interactions that help separate conformations. The scatter in the data also makes it clear that analysis of fragments for identification benefits in another way relative to precursor ion examination. With every fragment, there is another opportunity for the isomers to separate, providing 10-20 chances per peptide rather than just one.

In Figure 7c a histogram of the number of residues within which modifications were identified is shown. For most isomers, ATD overlaps pinpoint the exact site of modification (73%). Most of the remaining sites are identified within 2 residues (91%) and all are within 3 or 4. For most

peptides, the exact site of modification would be easily determined within these restrictions

because isomerization and epimerization do not occur at all residues with equal frequency. In

other words, if the narrowed site contained a single Ser or Asp residue, these would be the most

likely candidates for isomerization. For absolute verification, the narrowed list of candidates

would mean that a small number of synthetic peptides could be prepared to confirm the

modification assignment.
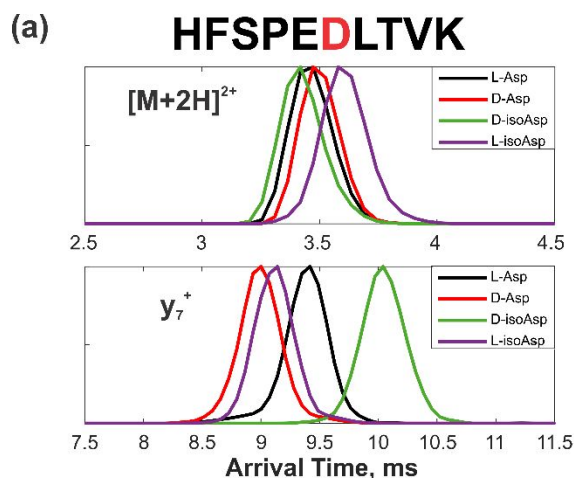
(a) HFSPEDLTVK

(b) ATDs Area-overlaps vs Fragment Sizes

(c)
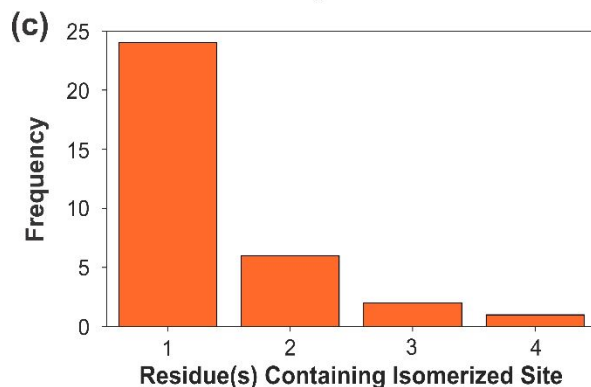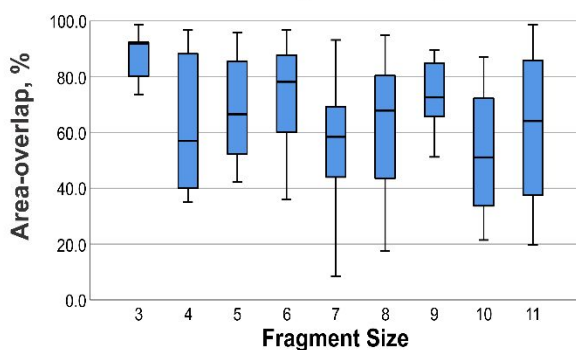
Figure 7(a) The ATDs of the precursor ions (top) and fragment ions y_7^+ (bottom) for the Asp

isomers of HFSPE<u>D</u>LTVK: L-Asp (Black), D-Asp (Red), D-isoAsp (Green), and L-isoAsp

(Purple). **(b)** Boxplot showing the ATD area-overlap values with respect to the fragment sizes.

(c) Histogram showing the distribution of the number of residues that contain the isomerized

site. One indicates the site is precisely determined. Two indicates the modification is within two

adjacent amino acids etc.

Conclusion

Our results demonstrate that ion mobility-based analysis of peptide isomers and epimers

holds great promise for the identification and localization of isomerized/epimerized sites.

Fragmentation of the peptides prior to ion mobility separation is beneficial both because it

creates a greater distribution of molecular sizes and increases the number of chances for

analysis. Isomer/epimer identification by comparison of ATD area overlap was successful for

every peptide examined. The more difficult task of modification site localization was also largely

achieved. In most cases, the precise residue can be located, in agreement with previous

reports.[29] For all peptides, the site could be localized within a few residues, narrowing the

possibilities significantly. When combined with knowledge of the biological propensity for

isomerization/epimerization, the data provided by this approach would most likely enable

synthesis of an authentic standard with a single attempt. In the worst case scenario, only a few

standards would be needed. These experiments were conducted on a commercially available

instrument that is accessible to many labs, but it also has relatively low mobility resolution.

Based on recent results demonstrating mobility-based separation of extremely similar species

such as isotopomers and isotopologues,[33] it is likely that higher resolution devices in the future

will be able to identify and localize isomerized sites with nearly perfect efficacy.

Supporting Information

21

Full CID mass spectra and the ATD area-overlaps and CID intensity ratios for the fragment ions of GYQYLLEPGDFR peptide isomers are provided.

Acknowledgements

References

---

[1] Lambeth, T. R.; Riggs, D. L.; Talbert, L. E.; Tang, J.; Coburn, E.; Kang, A. S.; Noll, J.; Augello, C.; Ford, B. D.; Julian, R. R. Spontaneous Isomerization of Long-Lived Proteins Provides a Molecular Mechanism for the Lysosomal Failure Observed in Alzheimer's Disease. *ACS Cent. Sci.* **2019**, *5* (8), 1387–1395.

[2] Lyon, Y. A.; Collier, M. P.; Riggs, D. L.; Degiacomi, M. T.; Benesch, J. L. P.; Julian, R. R. Structural and Functional Consequences of Age-Related Isomerization in α-Crystallins. *J. Biol. Chem.* **2019**, *294* (19), 7546–7555.

[3] Checco, J. W.; Zhang, G.; Yuan, W.; Yu, K.; Yin, S.; Roberts-Galbraith, R. H.; Yau, P. M.; Romanova, E. V.; Jing, J.; Sweedler, J. V. Molecular and Physiological Characterization of a Receptor for D-Amino Acid-Containing Neuropeptides. *ACS Chem. Biol.* **2018**, *13* (5), 1343–1352.

[4] Roher, A. E.; Lowenson, J. D.; Clarke, S.; Wolkow, C.; Wang, R.; Cotter, R. J.; Reardon, I. M.; Zurcherneely, H. A.; Heinrikson, R. L.; Ball, M. J. Structural Alterations in the Peptide Backbone of Beta-amyloid Core Protein May Account for its Deposition and Stability in Alzheimer's-disease. *J. Biol. Chem.* **1993**, *268* (5), 3072– 3083

[5] Toyama, B. H.; Savas, J. N.; Park, S. K.; Harris, M. S.; Ingolia, N. T.; Yates, J. R.; Hetzer, M. W. Identification of Long-Lived Proteins Reveals Exceptional Stability of Essential Cellular Structures. *Cell* **2013**, *154* (5), 971–982.

[6] Truscott, R. J. W.; Schey, K. L.; Friedrich, M. G. Old Proteins in Man : A Field in Its Infancy. *Trends Biochem. Sci.* **2016**, *41* (8), 654–664.

[7] Truscott, R. J. W.; Friedrich, M. G. The Etiology of Human Age-Related Cataract. Proteins Don't Last Forever. *Biochim. Biophys. Acta - Gen. Subj.* **2016**, *1860* (1), 192–198.

[8] Riggs, D. L.; Gomez, S. V; Julian, R. R. Sequence and Solution Effects on the Prevalence of D-Isomers Produced by Deamidation. *ACS Chem. Biol.* **2017**, No. 12, 2875–2882.

[9] Geiger, T.; Clarke, S. Deamidation, Isomerization, and Racemization at Asparaginyl and Aspartyl Residues in Peptides. *J. Biogical Chem.* **1987**, *262* (2), 785–794.

[10] Reissner, K. J.; Aswad, D. W. Deamidation and Isoaspartate Formation in Proteins: Unwanted Alterations or Surreptitious Signals? *Cell. Mol. Life Sci.* **2003**, *60* (7), 1281–1295.

[11] Bloemendal, H.; De Jong, W.; Jaenicke, R.; Lubsen, N. H.; Slingsby, C.; Tardieu, A. Ageing and Vision: Structure, Stability and Function of Lens Crystallins. *Prog. Biophys. Mol. Biol.* **2004**, *86* (3), 407–485.

[12] Lyon, Y. A.; Sabbah, G. M.; Julian, R. R. Differences in α-Crystallin Isomerization Reveal the Activity of Protein Isoaspartyl Methyltransferase (PIMT) in the Nucleus and Cortex of Human Lenses. *Exp. Eye Res.* **2018**, *171* (March), 131–141.

[13] Lyon, Y. A.; Sabbah, G. M.; Julian, R. R. Identification of Sequence Similarities among Isomerization Hotspots in Crystallin Proteins. *J. Proteome Res.* **2017**, *16* (4), 1797–1805.

[14] Livnat, I.; Tai, H. C.; Jansson, E. T.; Bai, L.; Romanova, E. V.; Chen, T. T.; Yu, K.; Chen, S. A.; Zhang, Y.; Wang, Z. Y.; et al. A D-Amino Acid-Containing Neuropeptide Discovery Funnel. *Anal. Chem.* **2016**, *88* (23), 11868–11876.

[15] Hooi, M. Y. S.; Truscott, R. J. W. Racemisation and Human Cataract. D-Ser, D-Asp/Asn and d-Thr Are Higher in the Lifelong Proteins of Cataract Lenses than in Age-Matched Normal Lenses. *Age (Omaha).* **2011**, *33* (2), 131–141.

[16] Riggs, D. L.; Silzel, J. W.; Lyon, Y. A.; Kang, A. S.; Julian, R. R. Analysis of Glutamine Deamidation: Products, Pathways, and Kinetics. *Anal. Chem.* **2019**, *91*, 13032–13038.

[17] Demarchi, B.; Collins, M.; Bergström, E.; Dowle, A.; Penkman, K.; Thomas-Oates, J.; Wilson, J. New Experimental Evidence for In-Chain Amino Acid Racemization of Serine in a Model Peptide *Anal. Chem.* **2013**, *85 (12),* 5835– 5842.

[18] Fujii, N.; Kawaguchi, T.; Sasaki, H.; Fujii, N. Simultaneous Stereoinversion and Isomerization at the Asp-4 Residue in BB2-Crystallin from the Aged Human Eye Lenses. *Biochemistry* **2011**, *50* (40), 8628–8635.

[19] Adams, C. M.; Kjeldsen, F.; Zubarev, R. A.; Budnik, B. A.; Haselmann, K. F. Electron Capture Dissociation Distinguishes a Single D-Amino Acid in a Protein and Probes the Tertiary Structure. *J. Am. Soc. Mass Spectrom.* **2004**, *15* (7), 1087–1098.

[20] Sargaeva, N. P.; Lin, C.; O'Connor, P. B. Identification of Aspartic and Isoaspartic Acid Residues in Amyloid Beta Peptides, Including A Beta 1-42, Using Electron-Ion Reactions. *Anal. Chem.* **2009**, *81* (23), 9778–9786.

[21] Tao, Y.; Julian, R. R. Investigation of Peptide Microsolvation in the Gas Phase by Radical Directed Dissociation Mass Spectrometry. *Int. J. Mass Spectrom.* **2016**, *409*, 81–86.

[22] Tao, Y.; Julian, R. R. Identification of Amino Acid Epimerization and Isomerization in Crystallin Proteins by Tandem LC-MS. *Anal. Chem.* **2014**, *86* (19), 9733–9741.

[23] Lambeth, T. R.; Julian, R. R. Differentiation of Peptide Isomers and Epimers by Radical-Directed Dissociation. In *Methods in Enzymology*; 2019; pp 67–87.

[24] Majuta, S. N.; Maleki, H.; Kiani Karanji, A.; Attanyake, K.; Loch, E.; Valentine, S. J. Magnifying Ion Mobility Spectrometry–Mass Spectrometry Measurements for Biomolecular Structure Studies. *Curr. Opin. Chem. Biol.* **2018**, *42*, 101–110.

[25] Pang, X.; Jia, C.; Chen, Z.; Li, L. Structural Characterization of Monomers and Oligomers. *J. Am. Soc. Mass Spectrom.* **2017**, 110–118.

[26] Jeanne Dit Fouque, K.; Garabedian, A.; Porter, J.; Baird, M.; Pang, X.; Williams, T. D.; Li, L.; Shvartsburg, A.; Fernandez-Lima, F. Fast and Effective Ion Mobility-Mass Spectrometry Separation of d -Amino-Acid-Containing Peptides. *Anal. Chem.* **2017**, *89* (21), 11787–11794.

[27] Zheng, X.; Deng, L.; Baker, E. S.; Ibrahim, Y. M.; Petyuk, V. A.; Smith, R. D. Distinguishing D- and l-Aspartic and Isoaspartic Acids in Amyloid β Peptides with Ultrahigh Resolution Ion Mobility Spectrometry. *Chem. Commun.* **2017**, *53* (56), 7913–7916.

[28] Nagy, G.; Kedia, K.; Attah, I. K.; Garimella, S. V. B.; Ibrahim, Y. M.; Petyuk, V. A.; Smith, R. D. Separation of β-Amyloid Tryptic Peptide Species with Isomerized and Racemized L-Aspartic Residues with Ion Mobility in Structures for Lossless Ion Manipulations. *Anal. Chem.* **2019**, *91* (7), 4374–4380.

[29] Jia, C.; Lietz, C. B.; Yu, Q.; Li, L. Site-Specific Characterization of d-Amino Acid Containing Peptide Epimers by Ion Mobility Spectrometry. *Anal. Chem.* **2014**, *86* (6), 2972–2981.

[30] Hood, C. A.; Fuentes, G.; Patel, H.; Page, K.; Menakuru, M.; Park, J. H. Fast Conventional Fmoc Solid-Phase Peptide Synthesis with HCTU. *J. Pept. Sci.* **2008**, *14*, 97–101.

[31] Bai, L.; Romanova, E. V.; Sweedler, J. V. Distinguishing Endogenous D-Amino Acid-Containing Neuropeptides in Individual Neurons Using Tandem Mass Spectrometry. *Anal. Chem.* **2011**, *83* (7), 2794–2800.

[32] Adams, C. M.; Zubarev, R. A. Distinguishing and Quantifying Peptides and Proteins Containing D-Amino Acids by Tandem Mass Spectrometry. *Anal. Chem.* **2005**, *77* (14), 4571–4580.

[33] Wojcik, R.; Nagy, G.; Attah, I. K.; Webb, I. K.; Garimella, S. V. B.; Weitz, K. K.; Hollerbach, A.; Monroe, M. E.; Ligare, M. R.; Nielson, F. F.; et al. SLIM Ultrahigh Resolution Ion Mobility Spectrometry Separations of Isotopologues and Isotopomers Reveal Mobility Shifts Due to Mass Distribution Changes. *Anal. Chem.* **2019**, *91* (18), 11952–11962.

For TOC only:

GYQY LLEPGD$_L$FR   GYQY LLEPGD$_D$FR

Arrival Time, ms